Structure of Southern Peru from Seismic Array Data Using Receiver Functions

Kristin Phillips, Rob W. Clayton, Paul Davis

Abstract

The subduction zone in southern Peru is imaged using converted phases from teleseismic P, PP, and PKP waves and P wave tomography using local and teleseismic events. The data comes from three linear arrays which have a total of almost 100 broadband seismic stations. The first array (Line 1) spans 300 km from the coast (Mollendo) to near Lake Titicaca (Juliaca) and is located in the normal dipping subduction regime. The second array (Line 2) runs from Juliaca to Cusco parallel to the oceanic trench and samples the transition from normal to flat subduction regimes. The third array (Line 3) is parallel to the first and runs from Nazca to Cusco in the shallow subduction region. The Moho is observed at a depth of up to 75 km beneath the Altiplano. At the mid-crustal level of 40 km, there is a continuous structure with a positive impedance contrast, which we suggest is the western extent of the Brazilian Craton as it under-thrusts to the west. Vp/Vs ratios estimated from receiver function stacks show an average value of about 1.75 for this region with some higher values near the volcanic arc, and some regions north of the line exhibit strong lateral variation in Vp/Vs. The results support a model of crustal thickening in which the margin crust is under-thrust by the Brazilian shield rather than delamination of lower crust through eclogitization. Results from the three arrays will allow for a comparison of the normal and flat subduction regimes, details of the transition between the two regimes, and the impact of the subducting Nazca Ridge on the subduction zone.

Introduction and Methods

Array Location

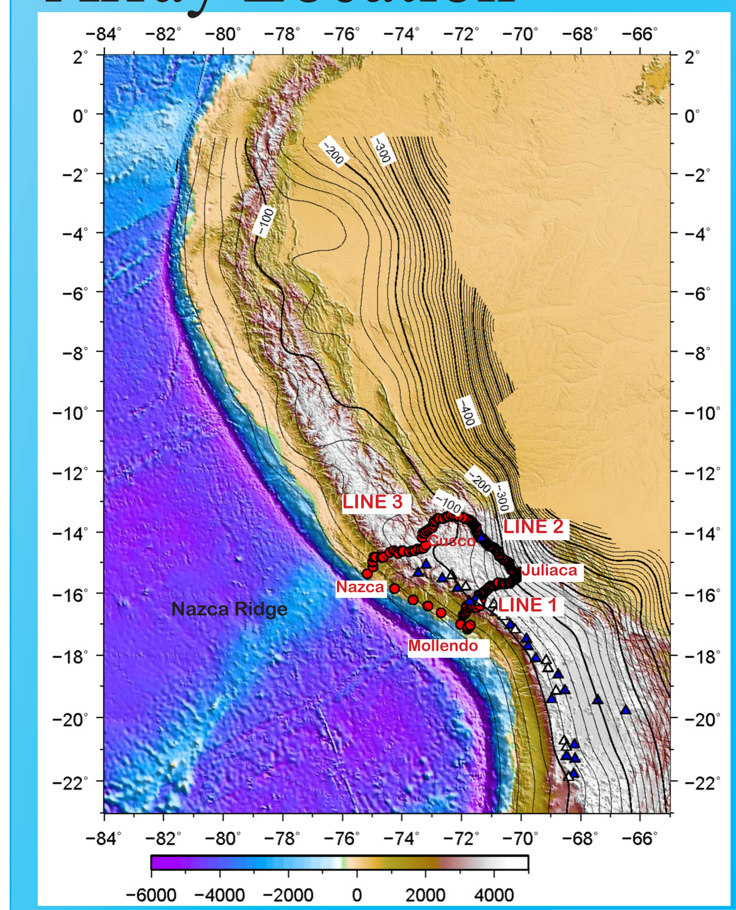

Topography and bathymetry of Peru showing the location of the subducting Nazca Ridge and the Altiplano of the central Andes. Variations in the dip angle of the Nazca plate can be seen through a contour model based on fits to seismicity. The locations of seismic stations installed in Peru as part of this study are denoted by red circles. Active and dormant volcanoes are denoted by blue and white triangles. The volcanic arc is located in the region of normal subduction dip angle in southern Peru while a volcanic gap is observable in the flat subduction regime in central and northern Peru.

Line 1: Samples normal dipping subduction region (~30 degree dip) from Mollendo to Juliaca

Line 2: Samples transition from normal to flat subduction between Juliaca and Cusco

Line 3: Samples flat subduction region near subducting Nazca Ridge between cities of Nazca and Cusco

Seismicity

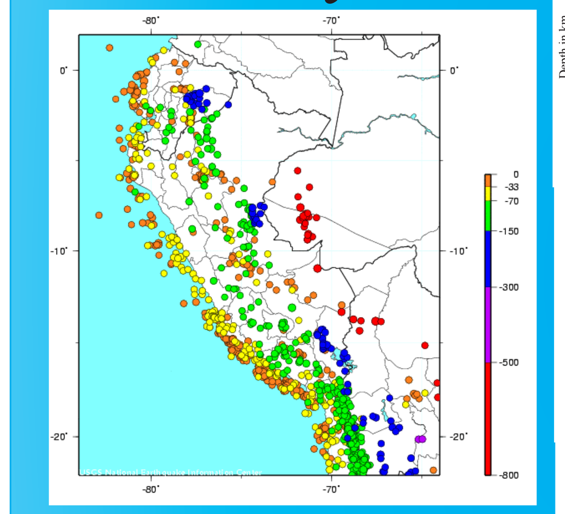

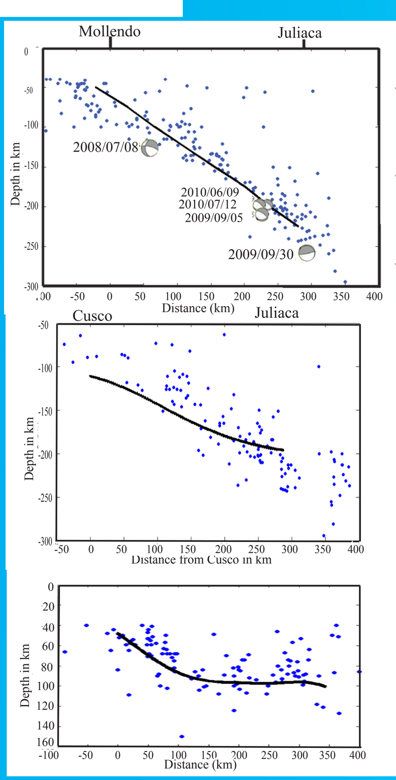

Far left: Map view of NEIC locations for local events in Peru

Line 1 seismicity depth cross section showing a slab dipping at around 30 degrees in the Southern-most region. Also shows some Harvard CMT solutions of events occuring near line

Line 2 Seismicity depth cross section showing the transition from normal subduction in the south to more shallow subduction regions to the north

Line 3 Seismicity depth cross section showing the slab flattening out at around 100 km which is characteristic of subduction in Northern and Central Peru.

Event Locations

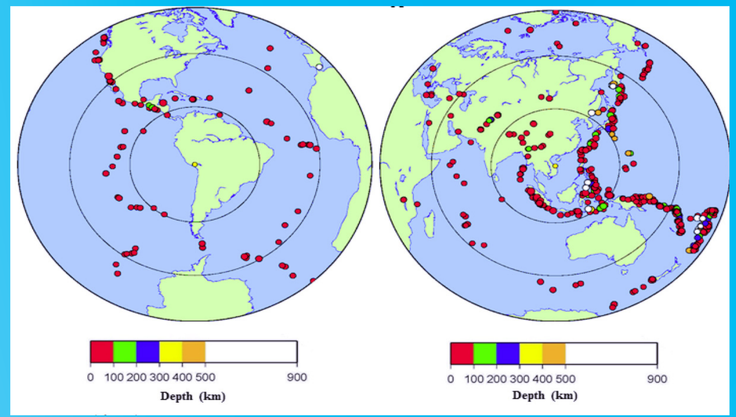

Event locations (events larger than ~M6.0 used for Line 1 analysis).
Left: Teleseismic events between 30 and 90 degrees distance from Peru were used to make P-wave receiver functions.
Right: Events greater than 90 degrees from Peru. The more distant events were used by studying converted arrivals of PP or PKP phases.

Receiver Functions

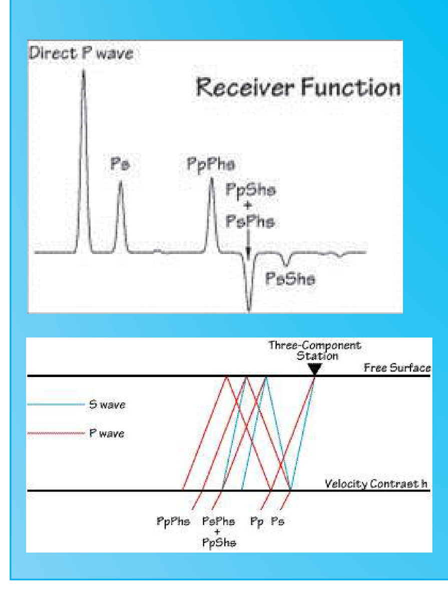

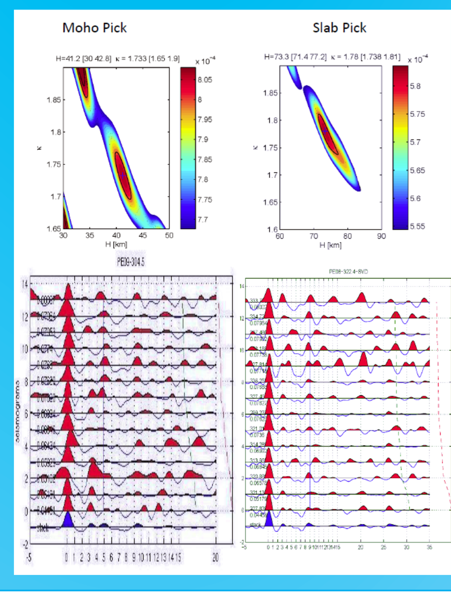

Receiver functions are formed using data from teleseismic events. P to S conversions occur at interfaces such as the Moho and the difference between the direct P and converted phases is related to the depth of the interface. Frequency domain deconvolution is performed. The radial component is deconvolved with the vertical to remove mantle propagation and source effects.

Receiver functions can be stacked for an individual station and the maximum summation for the converted phase and multiple arrivals can allow for estimates of interface depth (H) and Vp/Vs ratio (κ) using a grid search over a range of depths and velocity ratio values.

Results

Line 1

1

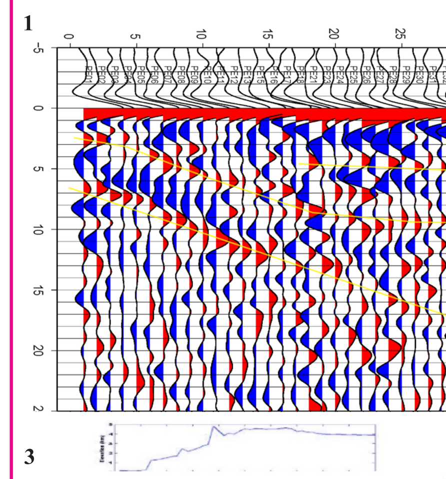

2

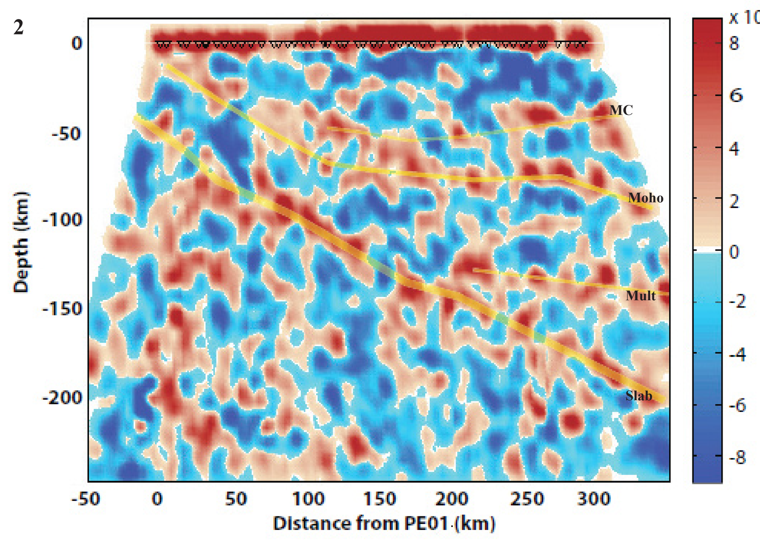

3

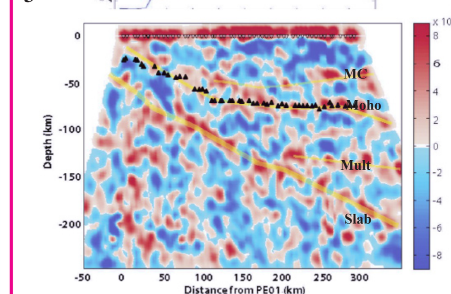

5

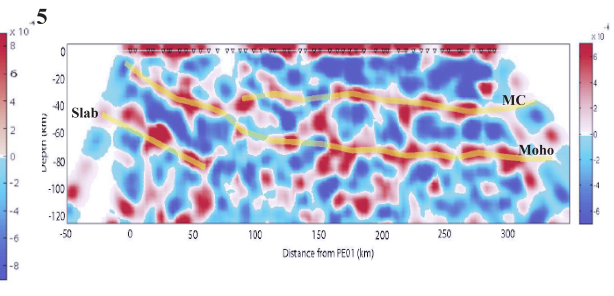

4

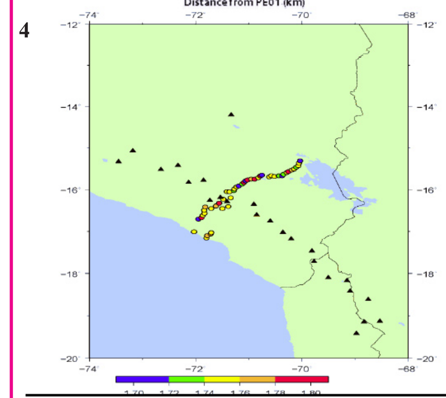

6

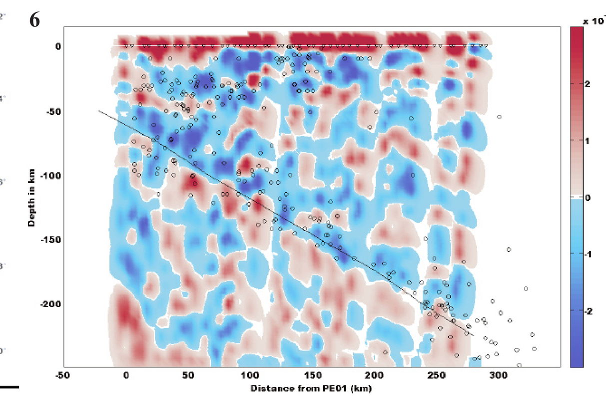

Receiver function images from Line 1 show a crustal thickness varying from around 20 km near the coast to about 75 km thickness beneath the Altiplano. Also visable is the subducting slab dipping at an angle of about 30 degrees (consistent with expectations from seismicity) and a positive impedance signal at around 40 km depth which is proposed to result from underthrusting of the Brazilian shield. Negative impedance signals observed at a depth of around 20 km could be indicative of magmatism.

1. Receiver function stacks for events coming from the NW azimuth to Peru. See description above for the major interfaces observed.

2. Receiver function image formed from backprojecting rays from the station in the direction from which the energy arrived. The signals for the mid-crustal structure, Moho, and slab are highlighted as well as a multiple arrival of the mid-crustal structure. This image includes only data from the NW azimuth.

3. Same image as 2 with the picks for the Moho based on stacking and grid search algorithm overlaid.

4. Vp/Vs ratio has an average of about 1.75. Higher values around the volcanic arc could indicate some degree of partial melting.

5. Upper 120 km based on data from all azimuths.

6. Image based on PKP phase using events from the Indonesian region. The slab can be seen clearly with the negative pulse corresponding to the top of the oceanic crust of the descending slab closely followed by a positive pulse at the transition to oceanic mantle. Because of the almost vertical arrival of these phases, a conversion is not expected at horizontal interfaces but the PKP arrivals can be useful for detecting dipping interfaces such as the slab.

Modeling Results

LEFT

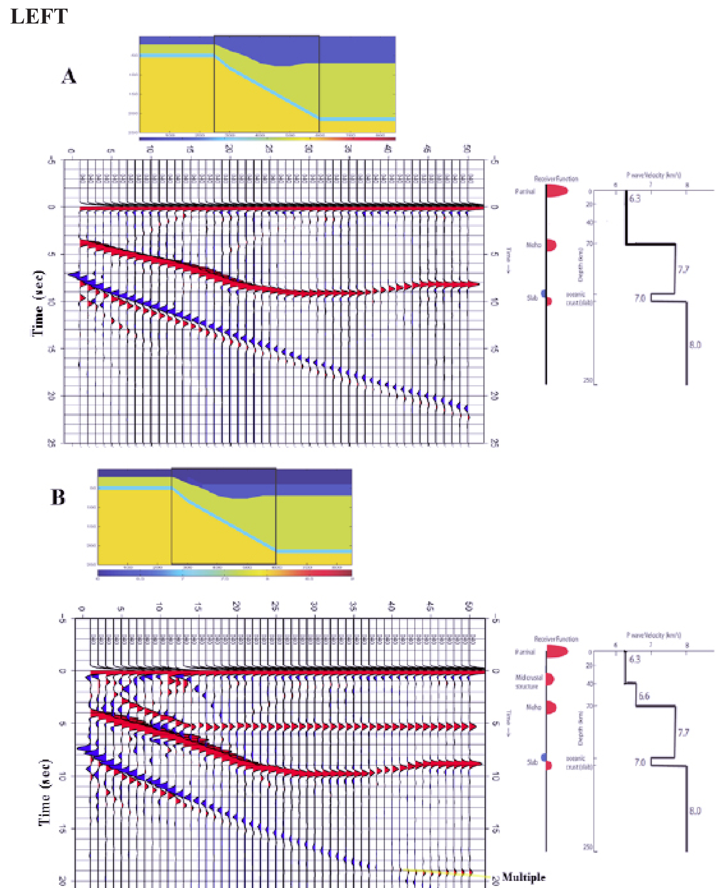

RIGHT

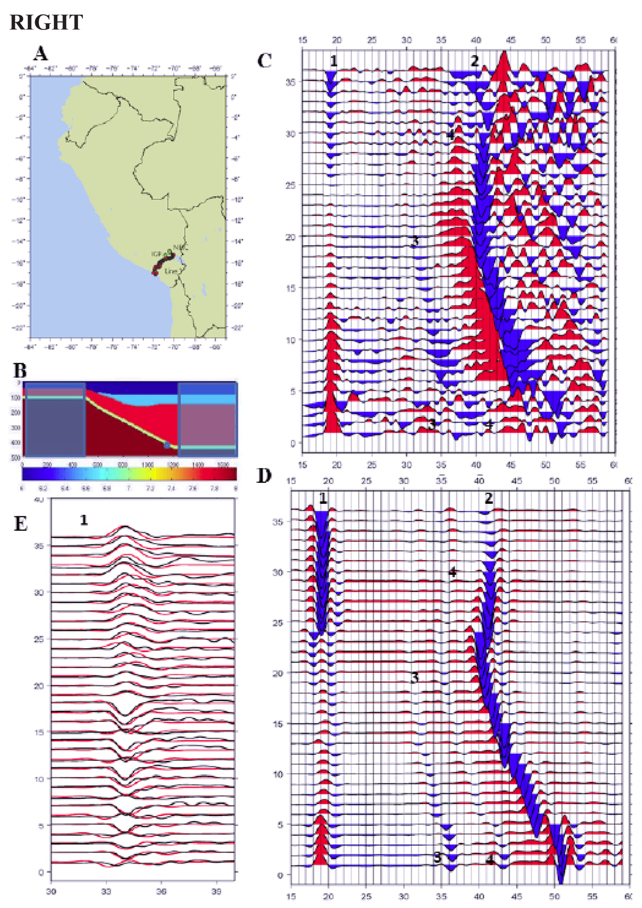

Left: Velocity model and synthetic receiver functions obtained from finite difference modeling. (A) Model with a homogenous crust (B) Model which includes a mid-crustal velocity jump which produces synthetics most consistent with observations.

Right: Local waveform finite difference modeling of local event near end of Line 1 (A) Map showing event locations provided by NEIC and IGP (Peru). (B) Model used in the finite difference modeling. (C) Data from a magnitude 6 event occurring on July 12, 2009 aligned by the P wave arrival. (D) Synthetics. (E) P wave arrival.

Arrivals are numbered: 1. P wave, 2. S wave, 3. Moho signal, 4. mid-crustal interface.

Line 2

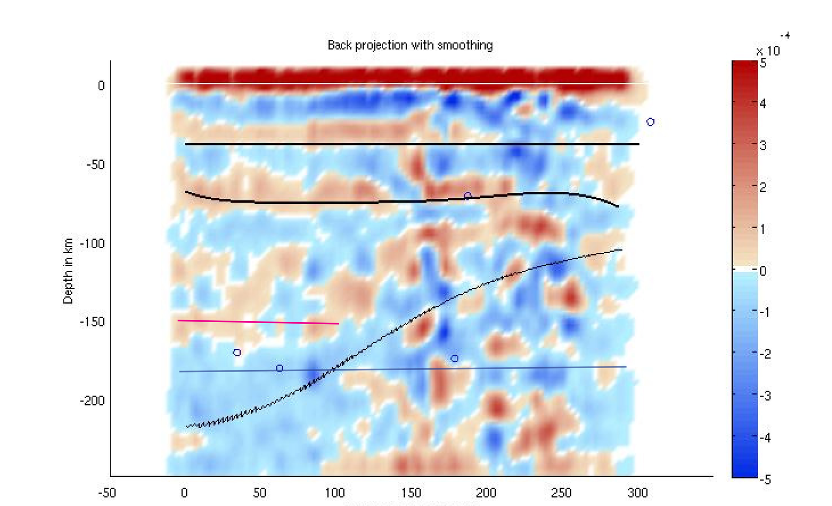

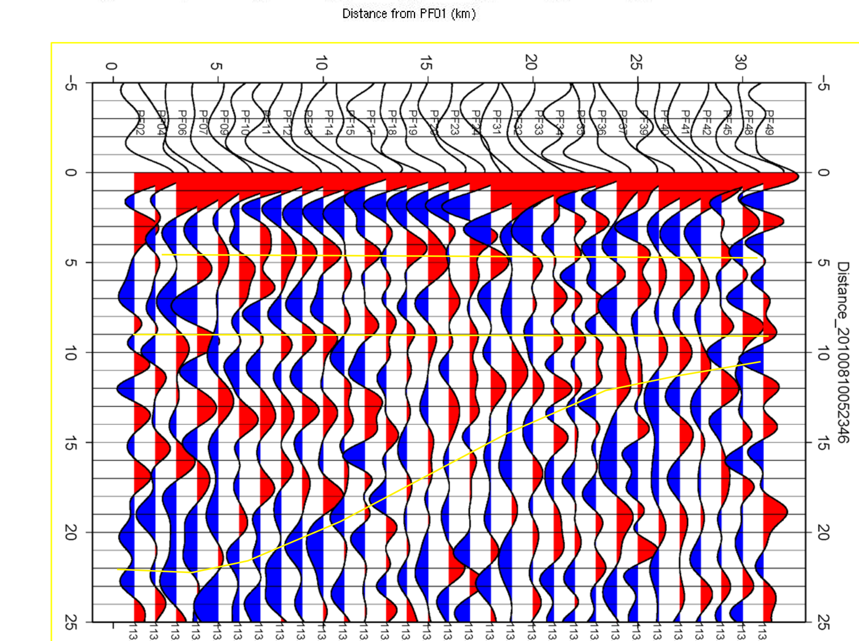

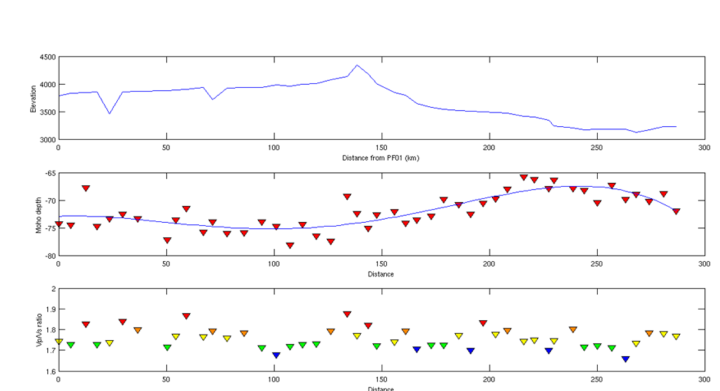

Receiver function results from Line 2 running from Juliaca/Lake Titicaca to Cusco and sampling the transition from normal subduction dip to shallow dip in the north. Results show a clear mid-crustal structure at around 40 km depth, a Moho at a depth of around 70 km depth, and a signal from the slab. Note that in some cases a clear slab double pulse signal is seen down to a depth of around 80-100km which may be related to the transport of hydrous minerals in oceanic crust into the subduction zone. This can be observed for Lines 1 and 3 but is less apparent for the deeper slab expected for Line 2.

Top: Receiver function image from common conversion point stack of all available data. Black lines delineate respectively from top to bottom the mid-crustal structure, Moho, and slab. Pink line shows the approximate location expected for the positive first multiple arrival of the mid-crustal structure and the blue line shows the expected location for the second (negative) multiple arrival.

Lower left: Receiver function from a signal Mw 7.3 event occuring on 8/10/2010 near Vanuatu.

Lower right: Estimates from receiver function stacking and grid search. Plotted are station elevation, Moho estimates fitted to a polynomial regression curve, and Vp/Vs estimates

Line 3

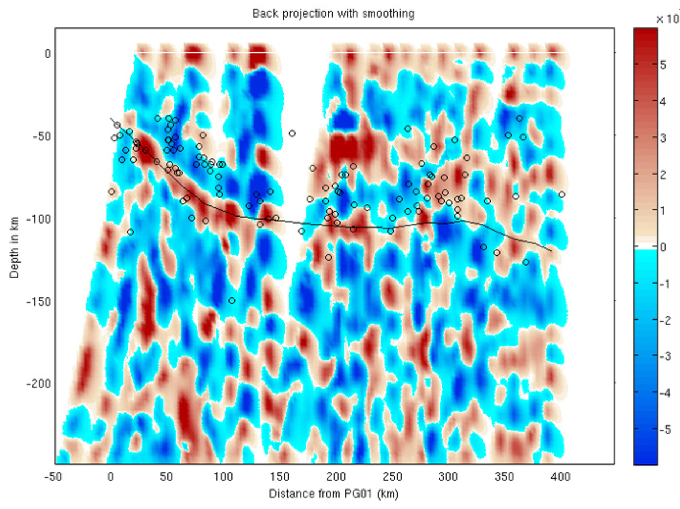

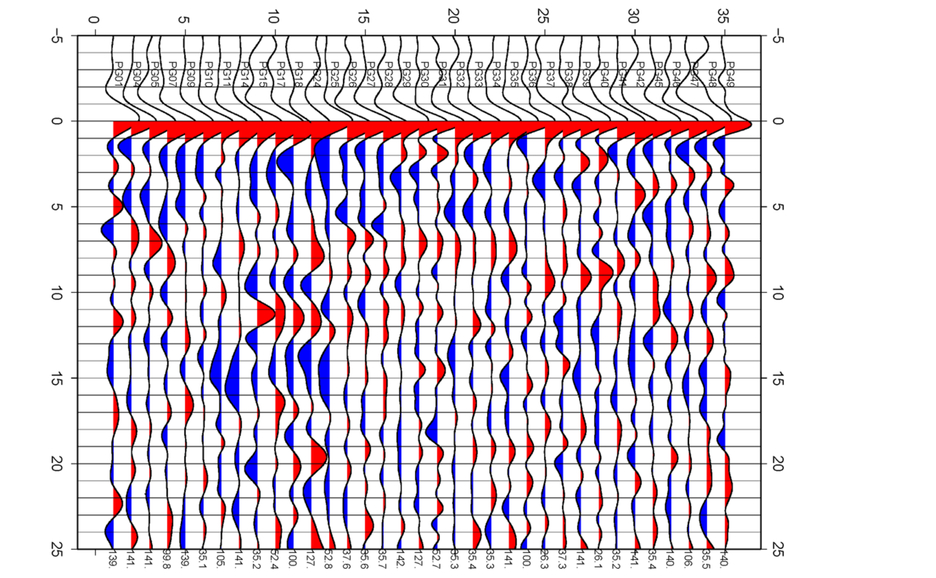

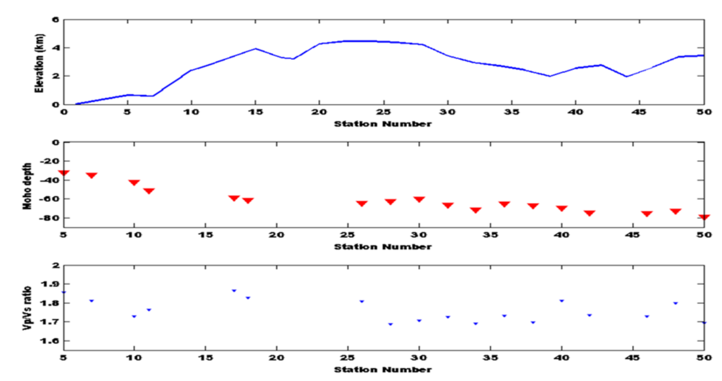

Receiver function results from Line 3 running from the city of Nazca near the coast to Cusco and sampling the flat subduction zone. The seismic array is perpendicular to the oceanic trench and is located near the subducting Nazca Ridge. The Nazca Ridge is proposed as a possible cause for flat slab subduction and results from this study may provide insight into the effects of the ridge on the subduction zone.

Top left: Receiver function image from events located at NW azimuth to Peru. The slab can be clearly seen flattening out at around 100 km depth. The Moho is located directly above the slab at a depth of around 70km.

Top right: Receiver functions from common conversion point (CCP) stack of available data.

Lower left: Estimates from receiver function stacking and grid search. Plotted are station elevation, Moho estimates, and Vp/Vs ratio estimates

Tomography

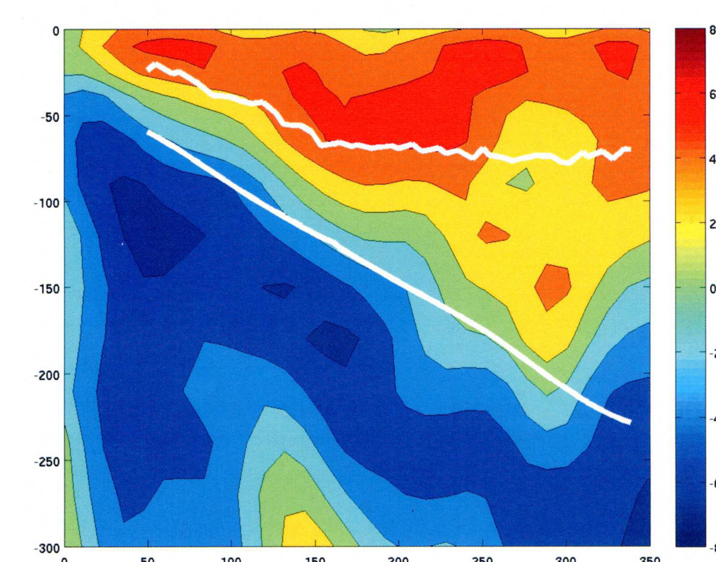

P wave tomography results beneath Line 1 as estimated by Paul Davis and researchers at UCLA. Deviations from the IASPEI model are in % slowness. The white lines represent receiver function estimates for the Moho and slab which are in agreement with tomography which shows a steeply dipping slab and a thick crust (around 75km thickness beneath the Altiplano). The low velocity to the right may be due to serpentinization of the mantle wedge, where eroded mantle lithosphere has been replaced by hydrated asthenosphere. Apparent slab thickening to the right and left of the model are artifacts from low resolution at the edges.

Implications

Uplift of Altiplano and Brazilian Shield Underthrusting

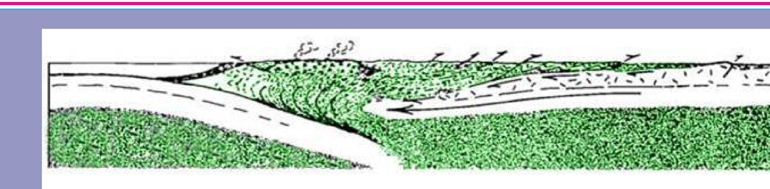

(Megard 1978)

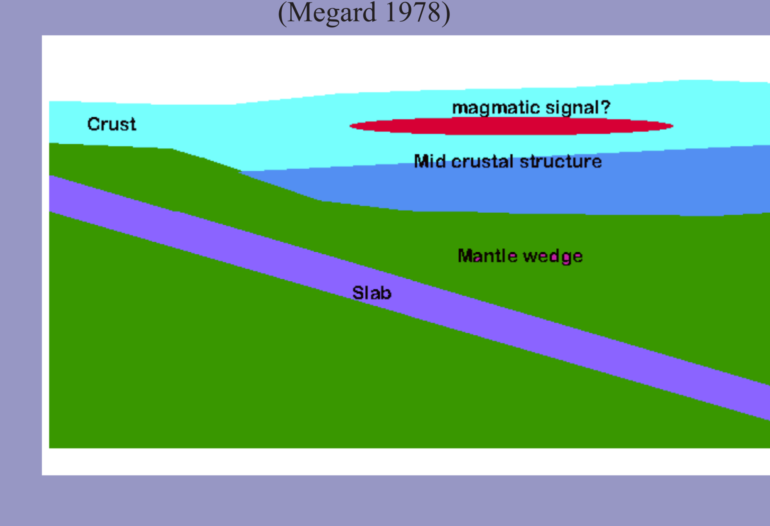

Positive impedance signal observed in the receiver function images at around 40km depth indicates mid-crustal velocity increase which we propose could represent Brazilian shield underthrusting beneath Altiplano. Previous authors have supported existence beneath Eastern Cordillera (McQuarrie et al., 2005; Gubbels et al., 1993; Lamb & Hoke, 1997; Beck & Zandt 02).

Presence of underthrusting shield has implications for timing of uplift of Altiplano. Two models proposed:
(1) Rapid uplift of about 2km over past 10Ma supporting mechanism of delamination (Gregory-Wodzicki, 2000; Garzione et al, 2006, 2008; Ghosh et al., 2006)

(2) Gradual rise over past 40km (Barnes and Ehlers, 2009; Ehlers and Poulsen, 2009; McQuarrie et al., 2005; Elger et al., 2005; Oncken et al., 2006)

It has also been suggested that there has been north/south variation in the mechanisms and rate of uplift so uplift in the Altiplano might have been different to that of the Puna plateau to the South (Allmendinger et al., 1996, 1997; Babeyko and Sobolev, 2005).

The underthrusting of the Brazilian shield is most consistent with the gradual rise model and the granulites with low water content of the shield are less likely to undergo eclogitization which occurs during delamination

Flat Slab subduction and the Nazca Ridge

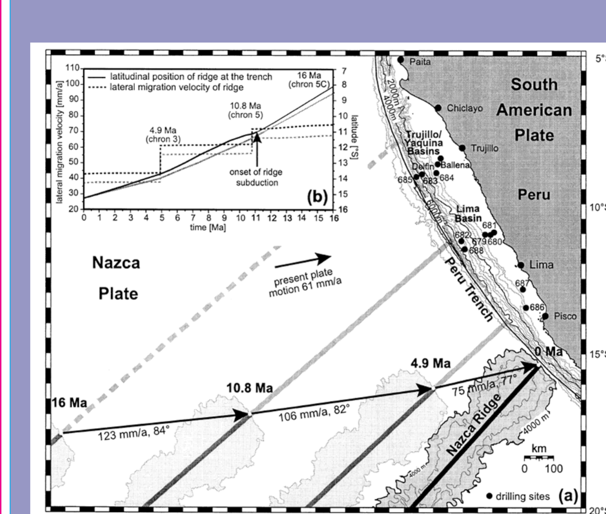

Proposed factors resulting in Peruvian flat slab subduction:

- Buoyancy from migrating Nazca Ridge flattening slab behind it
See image to left from Hampel, (2002) showing past positions of the Nazca Ridge.
The ridge is believed to have started subducting around 5Ma near Lima, Peru and migrated southward due to its oblique subduction angle. The ridge trends N42°E while the subduction angle between the Nazca and South American plates is about 77 degrees (Hampel, 02).
Receiver function results from Line 3 provides information about the impact of the Nazca Ridge on the subduction zone.

-Combined buoyancy of Nazca Ridge and hypothesized Inca Plateau (see cartoon figure to the right from Gutcher, 1999. Inca plateau is located in Northern Peru)

-Absolute motion of overriding South American plate

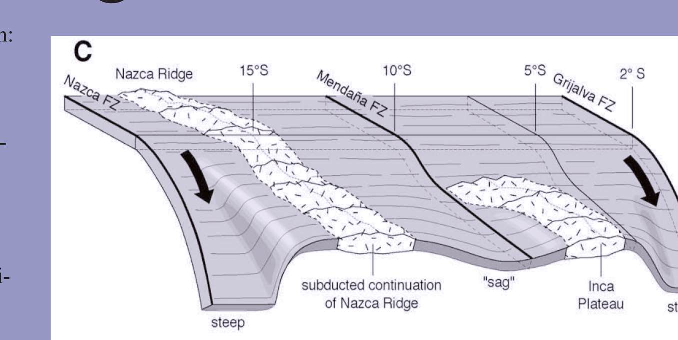

Other proposed factors involved in flat subduction:
-Age of subducting lithosphere

-Convex curvature of Peruvian margin

-Intraplate hydrostatic suction

Figure References:
- Phillips, K., R.W. Clayton, P. Davis, R. Guy, S. Skinner, I. Stubailo, L. Audin, V. Aguilar, H. Tavera, (2011) Structure of the Subduction System in Southern Peru From Seismic Array Data, In Preparation
- Hampel, A. (2002), The migration history of the Nazca Ridge along the Peruvian active margin: a re-evaluation, Earth and Planetary Science Letters, 203, 665–679.
- Gutscher, M., J. Olivet, D. Aslanian, J. Eissen, and R. Maury (1999), The “lost Inca Plateau”: cause of flat subduction beneath Peru?, Earth and Planetary Science Letters, 171 (3), 335–341.
- Megard F.. Etudes geologiques des Andes du Perou Central. Book (1978) pp. 1-315.

Acknowledgements: We thank the Betty and Gordon Moore Foundation for their support through the Tectonics Observatory at Caltech. This research was partially support by NSF award EAR-1045683.